Development of an ultra-high resolution diffraction grating for soft x-rays

Dmitriy L. Voronov*[a,b], Rossana Cambie[a], Ruslan M. Feshchenko[c], Eric M. Gullikson[a], Howard A. Padmore[a], Alexander V. Vinogradov[c], Valeriy V. Yashchuk[a]
[a]Lawrence Berkeley National Laboratory, Berkeley, California, 94720
[b]Kharkov Polytechnic University, Kharkov, Ukraine
[c]P. N. Lebedev Physical Institute, Moscow 119991, Russia

ABSTRACT

Resonant Inelastic X-ray Scattering (RIXS) is the one of the most powerful methods for investigation of the electronic structure of materials, specifically of excitations in correlated electron systems. However the potential of the RIXS technique has not been fully exploited because conventional grating spectrometers have not been capable of achieving the extreme resolving powers that RIXS can utilize. State of the art spectrometers in the soft x-ray energy range achieve ~0.25 eV resolution, compared to the energy scales of soft excitations and superconducting gap openings down to a few meV. Development of diffraction gratings with super high resolving power is necessary to solve this problem. In this paper we study the possibilities of fabrication of gratings of resolving power of up to 10^6 for the 0.5 – 1.5 KeV energy range. This energy range corresponds to all or most of the useful dipole transitions for elements of interest in most correlated electronic systems, i.e. oxygen K-edge of relevance to all oxides, the transition metal $L_{2,3}$ edges, and the $M_{4,5}$ edges of the rare earths. Various approaches based on different kinds of diffraction gratings such as deep-etched multilayer gratings, and multilayer coated echelettes are discussed. We also present simulations of diffraction efficiency for such gratings, and investigate the necessary fabrication tolerances.

Keywords: resonant inelastic soft X-ray scattering, high density grating, anisotropically etched silicon gratings, soft x-ray multilayers, sliced multilayer grating, spectral resolution.

1. INTRODUCTION

Resonant Inelastic X-ray Scattering (RIXS) is a relatively new probe of matter which can directly measure the energies of the soft excitations that are thought to be at the root of the complex properties of correlated electronic systems such as high T_c superconductors (for review, see Refs.[1-3] and references therein). Its main feature is that it is a spectroscopic probe that avoids limitations imposed by core hole lifetime energy broadening of conventional spectroscopies. Normally, the energy scale of soft excitations is significantly less than the energy broadening given by core hole lifetimes, and so are obscured from measurement. RIXS is a technique that scatters a photon in resonance with a core hole excitation off the valence states to be probed. That is a Raman-like process, when core excitation and decay are one coherent process, rather than independent events. The one-step scattering nature of the process avoids the normal spectroscopic energy broadening processes due to lifetime, and can reveal completely resolved energy loss features.

Many workshops around the world, including the international workshop 'Soft X-Ray Science in the Next Millennium' in the US in Pikeville TN,[4] have endorsed the RIXS approach to measuring the loss spectrum of complex materials. In this connection the workshop in Pikeville stated that "…the 'ultimate' instrumental requirements for frontier soft x-ray fluorescence and resonant inelastic scattering research include: 10-meV total energy resolution in the 100-eV to 5-keV photon energy range…" (Ref.[4], p. 45). This summarizes the issue; new methods must be found to achieve resolving powers up to 100 times that achieved now, but due to the small Raman x-ray cross section, these methods have to be highly efficient. Achieving such an improvement cannot be made with conventional grating optics because (i) it would dictate use of slit sizes that are extremely small; (ii) because of (i) almost all flux would be lost; (iii) extremely large spectrometers would be required, and (vi) because (i) and (iii) mean that unrealistically small optical slope errors would be required in the optics of the emission spectrometer.

*dlvoronov@lbl.gov, tel +1-510-495-4863

At the ALS Experimental Systems Group (ESG) in fiscal year 2007, we have started an LDRD (Laboratory Directed Research and Development) project to establish and demonstrate the technology required for ultra-high resolution RIXS with soft x-rays. The project addresses the basic issue of how to achieve resolving powers of 10^6 in a soft x-ray emission spectrometer using unconventional grating optics. It should be noted that such gratings would be useful not just for high resolution spectroscopy, but also for the temporal compression of chirped x-rays. A few approaches potentially suitable for fabrication of such a grating are discussed in Sec. 2. Fabrication of a grating for ultra-high resolution spectroscopy can be a challenging problem itself. In order to understand the range of tolerances and figure out the major requirements to the grating production technology, in Sec. 3 we perform analytical estimations of the effects of different possible distortion factors.

2. POSSIBLE APPROACHES TO FABRICATION OF A ULTRA-HIGH RESOLUTION DIFFRACTION GRATING FOR SOFT X-RAYS

There are two principle ways to achieve ultra-high spectral resolution in the soft X-ray wavelength range. One way is to use high order diffraction with a grating with reasonably low groove density, while another one is to use the first order diffraction of a grating with an ultra-high density of grooves.

A conventional grating, if it is used for high order x-ray diffraction, would provide very low diffraction efficiency, because for all normal reflecting materials, the scattering angle would need to be bigger than the critical angle of the material. The effective critical angle can be significantly increased with a multilayer (ML) coating.[5,6] In this case, the Bragg equation for the multilayer and the high order diffraction equation for the surface grating have to be simultaneously fulfilled. By choosing the appropriate set of multilayer and grating period parameters, it becomes possible to maximize diffraction efficiency for a selected high order. The lamellar ML grating, blazed ML grating, and sliced ML grating considered in Sec. 2.1 are the examples of such a grating.

Aiming for a resolving power in first diffraction order of 10^6 in a reasonably compact x-ray spectrometer assumes the need for 10^6 grating grooves with extremely high line density, ~50,000 l/mm. However, high quality conventional gratings, produced by mechanical ruling or ion etched into a mask produced by holographic lithography are limited to the groove density of around 5000 l/mm. We are developing a technique, discussed in Sec. 2.2, to fabricate a required high-density grating based on cutting a small period multilayer mirror at an oblique angle.

2.1 Gratings for high order diffraction of soft X-ray

Lamellar grating: Figure 1 shows a lamellar ML grating produced e.g., by ion beam etching of a multilayer deposited onto a flat substrate. It has previously been demonstrated that such a grating can provide high efficiency for the first order diffraction of hard x-rays with $\lambda = 0.154$ nm.[7,8] Here, we demonstrate that in order to increase the efficiency, the grating land has to be decreased and the grove depth has to be increased. This allows more multilayer periods to be involved in the diffraction process.

A high energy x-ray grating with highly asymmetrical s/d ratio was suggested and investigated and reported in the literature.[9] With $s/d = 0.2$, the diffraction efficiency of the desired first order was found to be ~95% of the 0th order; but at the same time, the efficiency of the second order was ~76%. As it was explained in,[9] for highly asymmetrical s/d ratios, the effective depth of the multilayer increases, and, therefore, more multilayers become involved in diffraction. As a result, the overlap of the multilayer diffraction orders reduces, and efficiency in a selected order can be enhanced.

The dependences of the diffraction efficiency of a soft x-ray grating ($\lambda = 12.4$ Å) on land-to-period ratio for the 5th and 9th orders are shown in Fig. 2. For the simulations we used a commercial code[10] that solves Maxwell's equations in 2d periodic structures; this code was validated to high precision against existing and proven differential theory methods of Neviere.[11] The grating under analysis was assumed to be made of an etched W/B4C multilayer with a total of 600 bilayers. Tungsten-to-bilayer thickness ratio was $\Gamma = 0.22$, with a period of 45 Å. The grating period was 4 μm.

The dependences in Fig. 2 have a characteristic oscillatory shape, strongly damped at larger land-to-period ratios. One can understand this behavior on the basis of light diffraction by a grating consisting of a succession of equidistant slits.[12] Relating this to a lamellar ML grating (Fig. 1), the diffracting slit element represents the grating land.

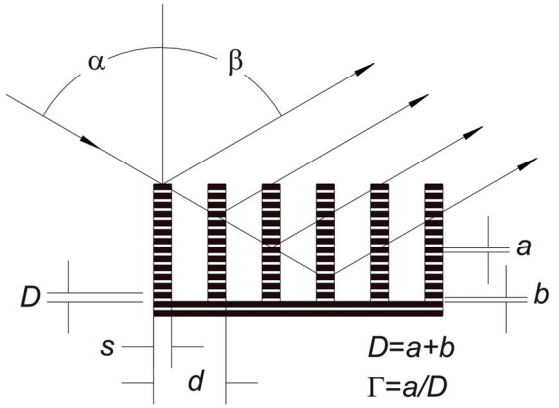

Fig. 1. Diffraction from a lamellar ML grating.

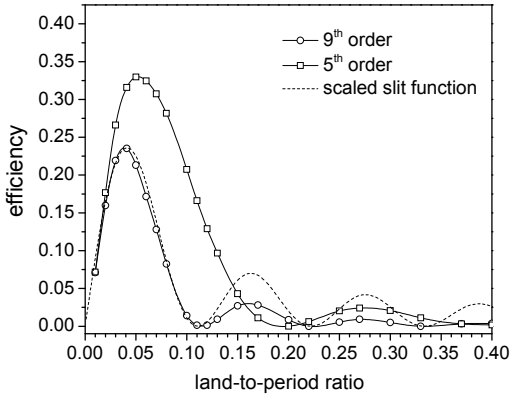

Fig. 2. Dependences of the diffraction efficiency of a soft x-ray ($\lambda = 12.4$ Å) grating on land-to-period ratio for the 5th and 9th orders. The period of the grating is 2 μm. The efficiency curve oscillations are predicted with the slit function shown with the dotted line.

Then, with the exact diffraction condition fulfilled,

$$Sin\alpha - Sin\beta = l\lambda/d \ , \tag{1}$$

the envelope of the normalized interference function, $I(l)$, called in[12] the light intensity function, can be written as

$$I(l) = I_0(\lambda, s, d, l, ...)R(\lambda, \alpha, N, ...)\,(s/d)\left[\,Sin(l\pi\, s/d)/(l\pi\, s/d)\,\right]^2 , \tag{2}$$

where $I_0(\lambda, s, d, l, ...)$ is the intensity normalization factor, $R(\lambda, \alpha, N, ...)$ is the reflectivity envelope function, accounting for finite reflection of the grating lands, l is the diffraction order. The term (s/d) in (2) can be thought of as a geometrical transmission factor of a slit. The function (2) envelopes the interference (diffraction) peaks, given by (1) at different l (see also discussion in Ref.[12]). The sinc function in the square brackets of (2) can be thought of as a result of the Fourier transform of an elementary slit. If $s/d = 0.5$, the odd, $(2l+1)$-th interference peaks are close to the l-th maxima of (2); whereas the even interference peaks, $(2l+2)$, are not observed, because their positions correspond to the zeros of the sinc function. However, if $s/d < 0.5$, the sinc function period increases, and the main peak of (2) starts to envelope the higher order interference peaks. In order to estimate the optimal (corresponding to the maximum diffraction efficiency) slit ratio, s/d, for a given l, we find the maximum of the product of two last terms in (2), $(s/d)\left[\,Sin(l\pi\, s/d)/(l\pi\, s/d)\,\right]^2$. The maximum reaches at $s/d \approx 1.166/(l\pi) \approx 0.371/l$ with the intensity in the maximum

$$I_{\max}(l) \approx I_0(\lambda, s, d, l, ...)R(\lambda, \alpha, N, ...)(4.34l)^{-1} . \tag{3}$$

The dotted line in Fig. 2 shows the slit function, scaled to fit the main peak of the calculated efficiency of 9th order diffraction. The function exactly predicts optimum for ratio s/d, emphasizing the point that to first order, the grating can be satisfactory described by a reflectivity function and a slit diffraction function.

Paradoxically, the agreement can be also thought of as an indication of the deviation of the grating, used for simulation, from an ideal one. Indeed, for a lamellar ML grating, the geometrical term can differ from that of a convectional grating.[13] For an ideal lamellar grating with significantly large number of bilayers (with no absorption), there should not be any geometrical losses. In this case, the maximum intensity, diffracted in high order, would be reached at infinitively small size of the grating lands, corresponding to the first maximum of sinc function in (2). However, any deviation from the ideality would be described with a geometrical loss factor, proportional (at least in first approximation) to the

parameter s. Such a loss would make appearance of the optimal finite size of the lands (slits), similar to that was found above.

The number of layers necessary for efficient diffraction has been also examined for the 9th order. From the simulation, it was found that approximately 1000 layer pairs are necessary to get maximum efficiency, and about 350 bilayers for the half of the maximum.

Concluding the discussion of possibility of use a lamellar ML grating in high order with soft x-rays, we should say that the efficiency of 9th order at $s/d \approx 0.05$ is rather high (Fig. 2), reaching close to the efficiency of the zero order. Small land width at large effective number of bilayers results to the separation of the orders (preventing overlapping). However, the reflectivity of a very narrow land is small, increasing the effective extinction length and demanding the large number of ML bilayers to provide high ML reflectivity and grating efficiency. As a result of that the optimal design has a very large aspect ratio that is a great challenge for existing lithographic technology.

Multilayer coated blaze (MLBG) grating[11] is another design of a low groove density grating, capable of providing high efficiency of diffraction in high orders (Fig. 3). The high efficiency of a MLBG grating in the 1st order has been demonstrated in EUV wavelength range.[14] In order to provide high efficiency of the grating in higher orders, a significantly larger blaze angle is required. This in turn has its limitations as the grating efficiency ultimately will be decreased due to enhanced shadowing and losses on non-working facets of the grating grooves.

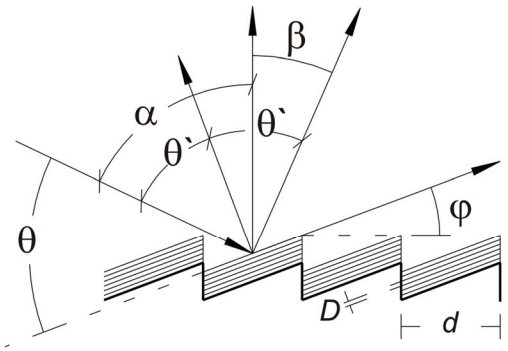

Fig. 3. Design of a multilayer coated blaze grating. d is the grating period, D is the ML bilayer spacing, φ is the blaze angle, α is the incidence angle, β is the diffraction angle, 2θ` is the scattering angle, θ is the Bragg angle.

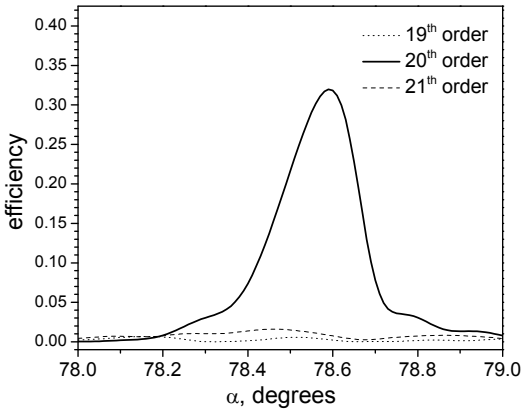

Fig. 4. Dependence of efficiency of 19th (the dotted line), 20th (the solid line), and 21th (the dashed line) diffraction orders of a MLCB grating on the incidence angle at 1.3 nm wavelength. The grating with the period d=1 μm and blaze angle ϕ=3.03° is optimized for 20th order. Parameters of W/B4C multilayer are: D_{ML}=2.644 nm, Γ=0.2, N=100. 30 orders were used in the calculation. The efficiency of the 20th order exceeds 30%, whereas the adjacent orders are almost completely suppressed due to high selectivity of the ML.

According to the Maystre - Petit scalar model[15], the resulting efficiency of a blaze grating is equal to the reflectivity of working facet, $R(\theta')$ multiplied by a geometry factor:

$$\frac{I_{\max}}{I_0} = R(\theta') \times \min\left(\frac{\cos\alpha}{\cos\beta}; \frac{\cos\beta}{\cos\alpha}\right). \tag{4}$$

The geometry factor increases at small scattering angle $2\theta'$, and reaches one at the Littrow geometry, when $2\theta' = 0^\circ$. The Littrow geometry works well for EUV range, where the reflectivity of ML mirrors at normal incidence can be rather high. In the soft x-ray range, the reflectivity of the ML mirrors rapidly decreases with increase of the grazing angle. In this case, the maximum efficiency for the chosen l-th order is achieved at some optimal value of scattering angle. Using the optimal scattering angle, grating equation, and Bragg equation, one can calculate all parameters of the grating,

including blaze angle, ML period, and angle of incidence, and estimate the grating efficiency. Figure 4 presents the results of optimization with the GSolver code of a MLBG grating for high efficiency diffraction of 1.3-nm x-rays in the 20th order. The optimized grating, with the period 1 μm and with the bilayer spacing of a W/B_4C multilayer of 2.644 nm, provides more than 30% efficiency at the blaze angle of 3.03°. Note that all other orders, including the zero order and nearest-neighbor ones, are significantly suppressed; so almost all diffracted energy is concentrated in the 20th order. It should be noted that the peak efficiency obtained in this detailed simulation is close to that obtained in the modification of the simple scalar model of Petit and Maystre.

2.2 Gratings with ultra-high density of grooves

A grating with very small period is an alternative possibility to achieve a high dispersive power and resolution. Such a grating can be fabricated by slicing and polishing the ML structure at some angle to the plane of the ML. This reveals the periodic structure with the period determined with the ML bilayer spacing and slice angle values. The grating equation and Bragg condition are fulfilled simultaneously, so the highest diffraction efficiency of the grating is achieved in first order, while the Bragg condition for the first order reflection from the ML structure is satisfied.

A high dispersive power of such a kind of grating fabricated by slicing the $MoSi_2$/Si ML at angle of 10 degrees, was experimentally demonstrated in EUV wavelength range.[16,17] However the number of grooves is the number of bilayers and it is difficult to exceed 10^3 due to deposition technique limitations; this obviously restricts the resolving power of the grating and its collection aperture. Moreover, as it will be shown below, the effect of an error in layer position increases with the number of a layer due to an accumulative effect that can impose a fundamental limitation of resolving power of this type of grating.

We propose a new design of sliced grating, which can provide the number of grooves as large as 10^6 and reasonably small size of the grating (2-10 cm). Such gratings can be fabricated by polishing of blaze ML gratings (Fig. 5). Simulations show that the efficiency of a sliced grating is determined by the ML reflectivity and appears to be larger than that of for a MLBG grating because of absence of the shadowing effect (Fig. 6).

The crucial point for both blazed MLBG gratings and sliced ML gratings is the quality of the saw-like tooth substrate. Surface roughness of the working facets can significantly decrease the efficiency of ML blaze grating.[18] The errors in the substrate periodicity as well as the accuracy of the ML period can affects both the efficiency and resolving power of the gratings. The tolerances of the grating substrate fabrication are discussed in the following section.

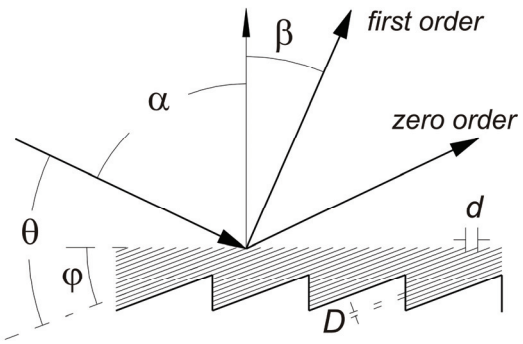

Fig. 5. Design of a sliced ML grating. The notations: d is the grating period, D is the ML bilayer spacing, ϕ is the slice angle, α is the incidence angle, β is the diffraction angle, θ is the Bragg angle.

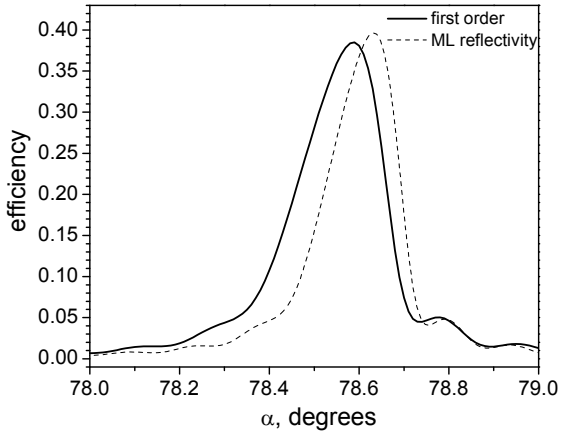

Fig. 6. Efficiency of a sliced multilayer grating (solid) as a function of incidence angle, at a wavelength of 1.3 nm, for the 1st grating order. The period of the grating with the slice angle ϕ=3.03° is d=50 nm. Parameters of W/B4C multilayer are the same as for blaze ML grating (Fig. 4): D_{ML}=2.644 nm, Γ=0.2, N=100. The efficiency of the sliced grating exceeds the one of the blaze grating due to the absence of shadowing, and is close to the ML reflectivity (dashed).

3. EFFECTS OF GROOVE'S PERIODICITY DISTORTION ON PERFORMANCE OF AN ULTRA-HIGH RESOLUTION DIFFRACTION GRATING

In this section in order to understand the range of tolerances and figure out the major requirements to the grating production technology, we estimate analytically the effects of different possible distortion factors. A grating with grooves normally distributed around their ideal positions is considered in Sec. 3.1. In Sec. 3.2, we analyzed an asymmetrically cut multilayer grating with normally distributed layers. The distortions considered in Sec. 3.1 and 3.2 are at the extremes of expected effect on grating performance. The requirements for production tolerancing of a grating according to Fig. 5 should be somewhere between the extremes. In this case consider in Sec. 3.3, the grating distortion associated with an error of period of the multilayer, which coats an ideal anisotropically etched Si substrate (echellette).

3.1 Grating with grooves normally distributed around their ideal positions

Let us consider a plane wave diffracted from a grating with uniformly distributed grooves, as in the case of a regular grating, or a multilayer structure, or in the case of a density grating formed by cutting a multilayer mirror at a small angle. Similar to an asymmetrically-cut-crystal, a single bilayer edge, seen as a line on the polished surface, can be considered as an elementary groove of the high density grating. In order to avoid limitation of the grating resolution by the number of groves, $N+1$, assume N to be large enough to provide the desired resolution. For simplicity, suppose an incident angle to be zero (normal incidence), $\alpha = 0^o$, Fig. 7. The grating diffracts the light at the angle β satisfying the grating equation with ideally uniform groove spacing d (l is an integer number, the order of diffraction),

$$l\lambda = d\,(Sin\,0^o + Sin\beta) = d\,Sin\beta\ . \tag{5}$$

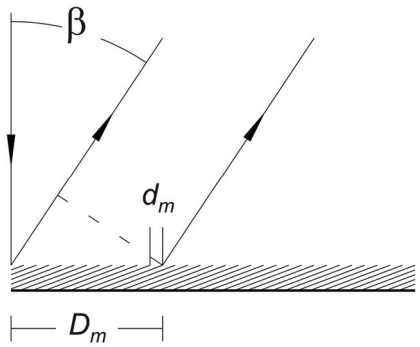

Fig. 7. Geometry of diffraction of a plane wave from a density grating formed by cutting a multilayer mirror at a small angle.

Suppose that the positions of the grooves D_m are normally distributed around their ideal positions $m\,d$ according to the Gaussian distribution law with dispersion σ_d^2:

$$P(\delta d_m) = \sqrt{2\pi\sigma_d^2}^{-1} \exp[-\delta d_m^2 / (2\sigma_d^2)], \quad \delta d_m = D_m - m\,d. \tag{6}$$

The electric field amplitude of the diffracted wave (normalized to the amplitude of the incident wave) can be thought of as a superposition of plane waves with the corresponding path differences calculated with respect to the first groove $(m = 0)$:

$$E = \frac{1}{(N+1)} \sum_{m=0}^{N} \exp[ikD_m Sin\beta] = \frac{1}{(N+1)} \sum_{m=0}^{N} \exp[ikSin\beta(md + \delta d_m)] = \frac{1}{(N+1)} \sum_{m=0}^{N} \exp[ikSin\beta\, m\,d] \exp[ikSin\beta\, \delta d_m], \tag{7}$$

where: δd_m is a deviation of the m-th groove from its ideal position, $k = 2\pi/\lambda$ is the wave number. Averaging of the electric field amplitude (7) with distribution (6) gives:

$$\widetilde{E} = (N+1)^{-1} \exp\left[-k^2 Sin^2\beta\, \sigma_d^2 / 2\right] \sum_{m=0}^{N} \exp[ikSin\beta\, m\,d]. \tag{8}$$

In order to get (8) we used a known expression for the Fourier transform (characteristic function) of the Gaussian distribution $P(x)$ (see, e.g. Ref.[19]),

$$\int_{-\infty}^{\infty} \exp[ikSin\beta\, x]P(x)\,dx = \exp\left[-k^2 Sin^2\beta\,\sigma_d^2/2\right]. \tag{9}$$

Using (8), a normalized intensity of the diffracted wave can be written as

$$\widetilde{E}\widetilde{E}^* \equiv Int = \frac{1}{(N+1)^2}\exp\left[-k^2 Sin^2\beta\,\sigma_d^2\right]\frac{Sin^2[kSin\beta\,(N+1)\,d/2]}{Sin^2[kSin\beta\,d/2]}. \tag{10}$$

Then, intensity at the exact diffraction conditions (5) is equal to

$$Int^{\max} = \exp\left[-k^2 Sin^2\beta\,\sigma_d^2\right], \tag{11}$$

that is smaller than 1 due to the groove's position perturbation.

In order to find the resolution of the grating, let us find the deviation from a given wave number δk such that intensity at $k+\delta k$ is half of the maximum intensity:

$$Int(k+\delta k) = Int_{\max}/2. \tag{12}$$

After algebraic and trigonometric transformation and accounting the exact diffraction condition (5), expression (12) gives:

$$\frac{1}{(N+1)^2}\exp\left[8\pi^2\frac{\delta\lambda}{\lambda}Sin^2\beta\frac{\sigma_d^2}{\lambda^2}\right]\frac{Sin^2[\delta k\,Sin\beta\,(N+1)\,d/2]}{Sin^2[\delta k\,Sin\beta\,d/2]} = \frac{1}{2}. \tag{13}$$

Because we are interested in a high-resolution grating, we can suggest that

$$\delta k\,Sin\beta\,d = 2\pi\left|\delta\lambda/\lambda\right|\cdot Sin\left(\beta\,d/\lambda\right) << 1 \quad \text{and} \quad 8\pi^2\left(\delta\lambda/\lambda\right)Sin^2\left(\beta\sigma_d^2/\lambda^2\right) << 1. \tag{14}$$

Then, equation (13) can be approximately solved, and the solution can be expressed as the grating resolution, equal to the full width of the diffraction peak on half of maximum, is

$$R = 2\left|\frac{\delta\lambda}{\lambda}\right| \approx \frac{2\cdot 1.39}{\pi\, l(N+1)} \approx \frac{1}{l\,N}. \tag{15}$$

Therefore, resolution for a grating with grooves normally distributed around their ideal positions and constructed according to condition (14) is equal to the resolution of an ideal grating with the same geometry. According to expression (11), the considered distortion of the grating leads to a reduction of intensity of the diffracted light. At

$$\sigma_d = d/(2\pi\, l), \tag{16}$$

the intensity would be reduced by factor of e. Note that the higher the order of diffraction used, the more precise fabrication of the grating has to be.

3.2 Asymmetrically cut multilayer grating with normally distributed layer thicknesses

In this section, we apply the analytical approach used in the previous section to a plane wave diffracted from a grating made of a multilayer structure asymmetrically cut (Fig. 8), similar to Ref.[16,17] A derivation analogous to one performed in Sec. 3.1 leads to a normalized intensity of the diffracted wave as

$$Int = \frac{1-2\exp(-k^2 Sin^2\beta\,(N+1)\sigma_d^2/2)Cos(kSin\beta\,(N+1)d) + \exp(-k^2 Sin^2\beta\,(N+1)\sigma_d^2)}{(N+1)^2\left\{1-2\exp(-k^2 Sin^2\beta\,\sigma_d^2/2)Cos(kSin\beta\,d) + \exp(-k^2 Sin^2\beta\,\sigma_d^2)\right\}}. \tag{17}$$

A maximum of intensity achieved at exact diffraction conditions (5) is

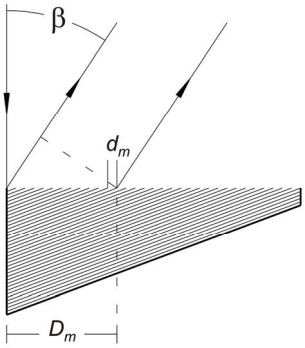

Fig. 8. Geometry of diffraction of a plane wave from a density grating formed by cutting a thick multilayer mirror at a small angle. We suppose that the thickness of the layers and, therefore, the d-factor of the grooves d_m are normally distributed with dispersion σ_d^2 around their mathematical expectation d according to the Gaussian distribution law (6), but now $\delta d_m = d_m - d$.

$$Int^{\max} = (N+1)^{-2} \cdot \left[1 - \exp(-k^2 Sin^2\beta\,(N+1)\,\sigma_d^2)\right]^2 \left[1 - \exp(-k^2 Sin^2\beta\,\sigma_d^2/2)\right]^{-2}. \qquad (18)$$

At sufficiently small σ_d^2, such that

$$k^2 Sin^2\beta (N+1)\,\sigma_d^2 = (2\pi/\lambda)^2 d^2 Sin^2\beta\,(N+1)\,\sigma_d^2/d^2 = (2\pi)^2 l^2\,(N+1)\,\sigma_d^2/d^2 << 2\,, \qquad (19)$$

the maximum intensity of the diffracted light is $Int_{\max} \approx 1$. From other hand, at sufficiently large $(N+1)$, such that

$$(2\pi)^2 l^2\,(N+1)\,\sigma_d^2/d^2 >> 2\,, \quad \text{while} \qquad (2\pi)^2 l^2\,\sigma_d^2/d^2 << 2\,, \qquad (20)$$

the maximum intensity of the diffracted light becomes much smaller than 1:

$$Int^{\max} \approx (N+1)^{-2}\left[1 - \exp\left(-k^2 Sin^2\beta\,\sigma_d^2/2\right)\right]^{-2} \approx (N+1)^{-2} \cdot \left(k^2 Sin^2\beta\,\sigma_d^2/2\right)^{-2} << 1\,. \qquad (21)$$

Dependence of maximum intensity $Int_{\max}$ of light diffracted into the first order ($l = 1$) on σ_d/d at different number of grooves $(N+1)$ given by equation (17) is shown in Fig. 9. In Fig. 9, the saturation at the higher relative accuracies (smallest values of σ_d/d) corresponds to the case when condition (19) is fulfilled. The linear (in log-log scale) slope corresponds to the conditions (20). The constant level ($\approx (N+1)^{-2}$) appearing at significantly lower accuracy ($\sigma_d/d \sim 1/2\pi$) corresponds to the situation when the structure does not work any more as a diffraction grating. Note that the conditions (20) are fulfilled for all interesting values of parameter σ_d/d.

The resolution of a grating with normally distributed size of grooves, we find from relation (12) with $Int(k+\delta k)$ given by (17), and $Int_{\max}$ given by (18). After algebraic and trigonometric transformation, it gives

$$(\delta k Sin\beta\, d)\exp[-(k+\delta k)^2 Sin^2\beta\,\sigma_d^2/4] = 1 - \exp[-k^2 Sin^2\beta\,\sigma_d^2/2]\ . \qquad (22)$$

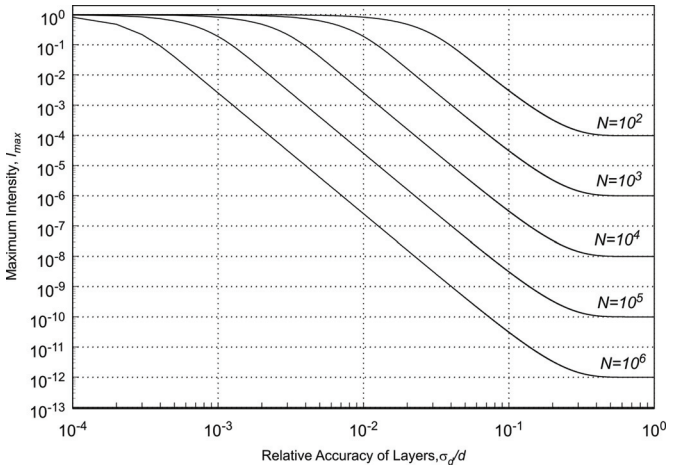

Fig. 9. Dependence of the maximum intensity $Int_{\max}$ on relative accuracy of the grating fabrication σ_d/d for different number of grooves $(N+1)$. $l = 1$. The saturation at the higher relative accuracies (smallest values of σ_d/d) corresponds to the case when condition (22) is fulfilled. The linear (in log-log scale) slope corresponds to the conditions (23). The constant level ($\approx N^{-2}$) appearing at significantly lower accuracy ($\sigma_d/d \sim 1/2\pi$) corresponds to the situation when the structure does not work anymore as a diffractive grating.

Because we are interested in a high-resolution grating, we can suggest that

$$2k\delta k\, Sin\beta\sigma_d^2 = -2(2\pi)^2(\delta\lambda/\lambda)Sin\beta\,\sigma_d^2/\lambda^2 \approx -8\pi^2(\delta\lambda/\lambda)Sin\beta\left(d^2/\lambda^2\right)\left(\sigma_d^2/d^2\right) << 1\,, \qquad (23)$$

Finally after simplification of (22) accounting for (23), the grating resolution is found to be

$$R = 2\left|\delta\lambda/\lambda\right| \approx 2\pi l\,\sigma_d^2/d^2\ . \qquad (24)$$

The result for the grating resolution (24) shows that high resolution for an asymmetrically cut multilayer grating with normally distributed layer thicknesses can be achieved only if the error of grating fabrication, determined as ratio σ_d/d is significantly small. Thus, in order to get resolution of $R \approx 10^{-6}$ at reasonable diffracted intensity, say, about 20-30%, the grating distortion has to be less than $\sigma_d/d < 10^{-3}$. Manufacturing of a multilayer grating with such accuracy is a challenging problem.

3.3 Polished Multilayer Coating on an Anisotropically Etched Substrate

Let us consider a plane wave diffracted from a grating shown in Fig. 10 and made by polishing of a multilayer structure, coating an ideal echellette - Fig. 5. Suppose an ideally sharp discontinuity of the multilayer coating appeared just on the edges of the echellette teeth, as it is shown in Fig. 10. In this case, the surface of the high-density grating has a periodic structure with period of the echellette, L. If the average multilayer period is p, the number of the multilayer grooves per L can be expressed in the terms of the averaged multilayer period, p, and blaze angle, φ:

$$n = L\,Sin\varphi/p = L/d\,, \qquad (25)$$

here d is the averaged groove spacing. Note that the total number n_0 of bilayers, coating the echellette, can significantly exceed n. However, it does not effect the performance of the grating under consideration.

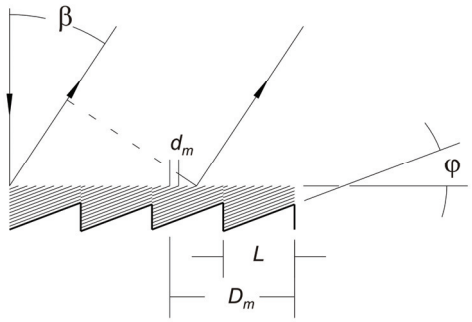

Fig. 10. Geometry of diffraction of a plane wave from a density grating formed by edges of the bilayers of a multilayer coating an echellette. L is the period of the echellette pattern on the substrate; D_m is the position of the $(m+1)$-th groove; φ is the blaze angle; β is the diffracting angle. The derivations in this section become clearer, if the groove numbering originates at the right-hand edge of the grating.

It is natural to assume the thickness of the bilayers and, therefore, the d-factor of the grooves d_m are normally distributed around their mathematical expectation d according to the Gaussian distribution law (6). Let the total number of grooves to be a multiple of n: $N+1 = M\,n$, where M is an integer number of the echellette teeth. Note that there is a variation of the total number of grooves n per the echellette period L, which is possible due to the variation of the bilayer thickness. However, we can ignore the variation of n without losing completeness of consideration because of the very small size of this last extra/missing bilayer at reasonable fabrication tolerances (compare with Fig. 10).

The grating in Fig. 10 diffracts the normal incidence light with wavelength λ at the angle θ satisfying the grating equation (5) with ideally uniform groove spacing d. The electric field amplitude of the diffracted wave is determined by the coordinate of the grooves D_m that can be presented as $D_m = md + \delta D_m = qL + (m-qn)d + \delta D_m$, where δD_m is the deviation of the position of the m-th groove from its ideal position, and q is the floor integer number of the ratio m/n. The deviation δD_m is a periodic function of period L of a discrete variable: $\delta D_{qn+s} = \delta D_s$. Such distortion of the grating period will lead to a ghost effect similar to the Rowland ghosts considered e.g., in ref.[20] In this work, in order to calculate the positions of the ghosts, the grating period error δD_m was expanded in a Fourier sine series and the diffraction result was obtained in terms of Bessel functions, convenient for ghost effect analysis. For our purpose,

because we are interested in simulation of the grating performance at the condition of the specified diffraction, we can use the same approach, as in the cases considered above, ignoring the ghost effect.

In this case, a normalized intensity of the diffracted wave can be written as

$$Int = \frac{1}{(N+1)^2} \times \frac{1 - Cos[kSin\beta\, n\, M\, d]}{1 - Cos(kSin\beta\, n\, d)} \times \frac{1 - 2\exp\left[-k^2 Sin^2\beta\, n\, \sigma_d^2/2\right] Cos[kSin\beta\, n\, d] + \exp\left[-k^2 Sin^2\beta n\, \sigma_d^2\right]}{1 - 2\exp\left[-k^2 Sin^2\beta\, \sigma_d^2/2\right] Cos(kSin\beta\, d) + \exp\left[-k^2 Sin^2\beta\, \sigma_d^2\right]}. \quad (26)$$

A maximum of intensity achieved at the exact diffraction condition (5) is

$$Int^{\max} = n^{-2} \cdot \left[1 - \exp\left(-k^2 Sin^2\beta\, n\, \sigma_d^2/2\right)\right]^2 \left[1 - \exp\left(-k^2 Sin^2\beta\, \sigma_d^2/2\right)\right]^{-2}. \quad (27)$$

Analysis of the obtained result can be performed in the way similar to one applied to the previously considered cases. First, suppose sufficiently small σ_d^2, such that $(2\pi)^2 l^2\, n\, \sigma_d^2/d^2 << 2$ [compare with (19)]; then the maximum intensity of the diffracted light is approximately equal 1. Whereas, at sufficiently large n, such that $(2\pi)^2 l^2\, n\, \sigma_d^2/d^2 >> 2$, while $(2\pi)^2 l^2\, \sigma_d^2/d^2 << 2$ [compare with (20)], the maximum intensity of the diffracted light becomes much smaller than 1. In this limit, expression for the intensity of the diffracted wave is identical to one obtained in sec. 3.2, Eq. (21). The only difference is the number of grooves, contributing to the accumulation of error of the grating period, n rather than $N+1$ in Eq. (21). It is an expected result, because the distortions considered in Sec. 3.1 and Sec. 3.2, are, indeed, the particular cases of the distortion investigated here, when $M = N+1$, $n = 1$ and when $M = 1$, $n = N+1$, respectively. Similarly, the dependence of the maximum intensity $Int_{\max}$ of light diffracted into the first order ($l = 1$) on the ratio σ_d/d at different number of grooves per an echellette tooth, n, given by (25), is the same as one shown in Fig. 9, if one replaces N in Fig. 9 with n. Similar to other considered cases, the resolution of a grating with normally distributed spacing of bilayers on an ideal echellette, we find from relation $Int(k + \delta k) = 0.5 \cdot Int_{\max}$ with $Int(k + \delta k)$ given by (26), and $Int_{\max}$ given by (27). After algebraic and trigonometric transformation, accounting $\delta k/k << 1$, $2\pi^2 l^2\, \sigma_d^2/d^2 << 1$, the exact diffraction condition $k\, Sin\beta\; d = 2\pi l$, corresponding to wave number k, one can get an equation suitable for analysis:

$$\begin{aligned} &(1/2 + \delta k/k)\left[1 - \exp(-2\pi^2 l^2\, n\, \sigma_d^2/d^2)\right] \approx Sin^2\left(\pi l\, n\, M\, \delta k/k\right)\left(\pi l\, n\, M\, \delta k/k\right)^2 \times \\ &\left[1 - \exp(-2\pi^2 l^2\, n\, \sigma_d^2/d^2) + \left(4\pi^2 l^2\, n\left(\sigma_d^2/d^2\right)\delta k/k\right)\exp(-2\pi^2 l^2\, n\, \sigma_d^2/d^2)\right] \end{aligned} \quad (28)$$

Using the approximation

$$2\pi^2 l^2\, n\, \sigma_d^2/d^2 << 1, \quad (29)$$

equation (28) gives the resolution estimation identical to Eq. (15) obtained in Sec. 3.1 for a grating with grooves normally distributed around their ideal positions and corresponds to an ideal grating. Therefore, in order to get a high-resolution grating we should fulfill the condition (29) that establishes the requirement for the fabrication of the grating:

$$\sigma_d/d << \left(\sqrt{2n}\, l\pi\right)^{-1}. \quad (30)$$

For first order diffraction, $l = 1$, and a reasonable number of bilayers, $n = 100$, the required relative accuracy of a bilayer thickness is about 2%. That is a very reasonable criterion for current coating technology.

4. DISCUSSION AND CONCLUSION

In the present work, we have considered a few approaches to fabricate an ultrahigh resolution soft x-ray grating with resolving power up to 10^6. Such a grating would enable an optimum use of the high resolution Resonant Inelastic X-ray Scattering technique with soft x-rays, at a resolution appropriate for examining the soft excitations that drive such phenomena as high temperature superconductivity. It should also be noted that this type of ultrahigh resolution grating can also be used for the temporal compression of long pulses. The path length difference introduced by the grating is simply the number of grooves multiplied by the wavelength. In this case, for example at 10 nm wavelength, this would

be 10 mm, leading to ~30-psec chirping time. Chirping of the position/angle/energy of the beam in time in combination with use of such a grating could allow significant temporal compression.

We have also analyzed the effect of possible distortions of the grating periodicity on diffraction efficiency. More detailed derivations can be found in Refs.[21-23] It was shown that a grating, suggested here and made of an asymmetrically polished multilayer coating on an ideal anisotropically etched substrate (echellette), allows one to significantly weaken the tolerance for the multilayer fabrication. This becomes possible due to an effective periodic 'tuning' of positions of the grating grooves by the echellette. Analytically and with scalar numerical calculations, we have demonstrated that an extremely high diffracted intensity of more than 50% and resolution of about 10^{-6} are in principal possible with such a grating fabricated with relative error of about 1%. The fabrication error mainly affects the diffracted intensity. It can be illustrated with Fig. 11, which shows the dependence on the number of bilayers n of maximum intensity of a wave diffracted into $l = 1$ order by a grating coated with relative accuracy of 1%. At this tolerance, the intensity of the diffracted wave is about 50% at approximately 400 bilayers.

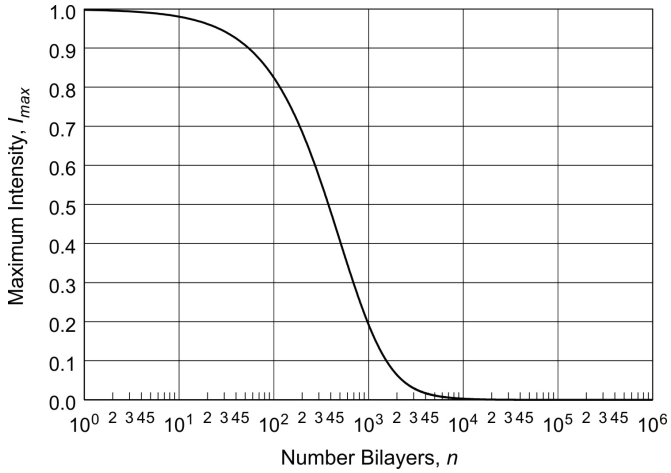

Fig. 11. Dependence of maximum intensity of a wave diffracted in the first order by a grating coated with relative accuracy of 1% on number of bilayers coated an ideal echellette. Total number of grooves is 10^6.

In the above consideration, the incident angle was chosen to be zero (normal incidence). For another incident angle, a similar derivation could be performed leading to a similar result. Moreover, qualitatively, the obtained result can be easily confirmed with the Fourier transform of the grating profile. After the Fourier transformation, a normal distribution of the grooves around their ideal position would manifest itself as an increased background, independent of any specific frequency.

Note that, strictly speaking, the results obtained in the present work are valid only for diffraction by the grating surface and only for scalar considerations without accounting for the possible effects which would appear in a more sophisticated vector theory. The effect of the multilayer structure, especially important for the case of x-ray diffraction, is also not accounted. However, we believe that the estimation gives the right order of the perturbation effects even for the case of volume diffraction. More detailed simulations, accounting this and other issues, are in progress. Finally it should be noted that we have embarked on production of the required grating substrates, using existing techniques of anisotropic etching of asymmetrically cut Si(111) and obtained blazed substrates of high quality. We will further optimize the substrate production and then multilayer coat these substrates in the near future.

5. ACKNOWLEDGEMENTS

The authors are grateful to W. McKinney and T. Warwick for extremely useful discussions. This work was supported by the U. S. Department of Energy under contract number DE-AC02-05CH11231.

6. DISCLAIMER

Certain commercial equipment, instruments, software, or materials are identified in this document. Such identification does not imply recommendation or endorsement by the US Department of Energy, LBNL or ALS nor does it imply that the products identified are necessarily the best available for the purpose.

REFERENCES

1. S. Eisebitt, W. Eberhardt, *Band structure information and resonant inelastic soft X-ray scattering in broad band solids,* J. El. Spec. Rel. Phen. 110-111(1-3), 335-58 (2000).
2. A. Kotani, S. Shin, *Resonant inelastic X-ray scattering spectra for electrons in solids*, Rev. Mod. Phys. 73(1), 203-46 (2001).
3. M. Altarelli, *Resonant X-ray scattering: a theoretical introduction,* in: Magnetism: A Synchrotron Radiation Approach (Springer-Verlag. 2006), pp. 201-42.
4. Workshop on "*Soft X-Ray Science in the Next Millennium: The Future of Photon-In/Photon-Out Experiments.* (Pikeville, Tennessee March 15–18, 2000), http://www.phys.utk.edu/WPWebSite/ewp_workshop_X-Ray_Report.pdf.
5. T. W. Barbee, Jr., *Combined microstructure X-ray optics,* Rev. Sci. Instrum. 60(7), 1588-95 (1989).
6. W. K. Warburton, *On the diffraction properties of multilayer coated plane gratings*, Nucl. Instrum. Meth. A291(1-2), 278-85 (1990).
7. A. I. Erko, B. Vidal, P. Vincent, Yu. A. Agafonov, V. V. Martynov, D. V. Roschupkin, M. Brunel, A. *Multilayer grating efficiency: numerical and physical experiments*, Nucl. Instrum. Meth. 333(2-3), 599-606 (1993).
8. V. Martynov, B. Vidal, P. Vincent, M. Brunel, D. V. Roschupkin, Yu. Agafonov, A. Erko, A. Yuakshin**,** *Comparison of modal and differential methods for multilayer gratings*, Nucl. Instrum. Meth. 339(3), 617-25 (1994).
9. V. V. Martynov, H. A. Padmore, V. Yakshin, Yu. A. Agafonov., *Lamellar multilayer gratings with very high diffraction efficiency*, Proceedings of the SPIE 3150, pp. 2-8 (1997).
10. D. Fluckiger, GSolver V4.2: Diffraction grating analysis program, 2005 (*www.gsolver.com)*.
11. M. Neviere, F. Montiel, *Soft x-ray multilayer coated echelle gratings: electromagnetic and phenomenological study*, J. Opt. Soc. Am. A, 13(4), 811-818 (1996).
12. M. Born, and E. Wolf, *Principles of Optics,* seventh edition (University Press, 2003), p. 459.
13. H. W. Schnopper, L. P. Van Speybroeck, J. P. Delvaille, A. Epstein, E. Kallne, R. Z. Bachrach, J. Dijkstra, L. Lantward, *Diffraction grating transmission efficiencies for XUV and soft x rays,* Applied Optics 16(4) 1088-91 (1977).
14. P. P. Naulleau, J. A. Liddle, E. H. Anderson, E.M. Gullikson, P. Mirkarimi, F. Salmassi, E. Spiller, *Fabrication of high-efficiency multilayer-coated gratings for the EUV regime using e-beam patterned substrates*, Opt. Communications, 229, 109-116 (2004).
15. D. Maystre, and R. Petit, *Some recent theoretical results for gratings; application for their use in the very far ultraviolet region*, Nouv. Rev. Opt., **7**, 165-180, (1976).
16. V. E. Levashov, E. N. Zubarev, A. I. Fedorenko, V. V. Kondratenko, O. V. Poltseva, S. A. Yulin, I. I. Struk, A. V. Vinogradov, *High throughput and resolution compact spectrograph for the 124-250A range based on $MoSi_2$-Si sliced multilayer grating,* Optics Communications 109, 1-4 (1994).
17. R. M. Fechtchenko, A. V. Vinogradov, and D. L. Voronov, *Optical properties of sliced multilayer gratings,* Optics Communications 210, 179-186 (2002).
18. Underwood, J.H., et al., Multilayer-*coated echelle gratings for soft x rays and extreme ultraviolet*, Rev. Sci. Instrum. 66(2), 2147-2150 (1995).
19. R. N. Bracewell, *The Fourier Transform and its applications*, third edition (Tata McGraw-Hill, 2003).
20. J. A. E. Calatroni and M. Garavaglia, *New Analysis of the Theory of Rowland Ghosts*, Applied Optics 12(10), 2298-2301 (1973).
21. R. Feshchenko, D. L. Voronov, V. V. Yashchuk, *Estimation of Effect of Groove's Periodicity Distortion on Performance of a Diffraction Grating; Part 1: Grating with grooves normally distributed around their ideal positions,* Light source Note LSBL-816 (February, 2007).
22. R. Feshchenko, D. L. Voronov, V. V. Yashchuk, *Estimation of Effect of Groove's Periodicity Distortion on Performance of a Diffraction Grating; Part 2: Asymmetrically Cut Multilayer Grating with Normally Distributed Layer Thicknesses*, Light source Note LSBL-817 (February, 2007).
23. V. V. Yashchuk, R. Feshchenko, A. V. Vinogradov, D. L. Voronov, H. A. Padmore, *Estimation of Effect of Groove's Periodicity Distortion on Performance of a Diffraction Grating; Part 3: Polished Multilayer Coating on Anisotropically Etched Substrate*, Light source Note LSBL-840 (June, 2007).